The Journal of Chemical Physics

RESEARCH ARTICLE | NOVEMBER 01 1983

A generalized van der Waals model for solvation forces between solute particles in a colloidal suspension

Ben C. Freasier; Sture Nordholm

Check for updates

J. Chem. Phys. 79, 4431–4438 (1983)
https://doi.org/10.1063/1.446328

View Online Export Citation

Articles You May Be Interested In

Coupling effect of solvent–colloid interaction on diffusivity and viscosity of colloidal hard-sphere suspensions: Statistical mechanical free-volume approach

Physics of Fluids (August 2023)

Nano-dewetting: Interplay between van der Waals- and short-ranged interactions

J. Chem. Phys. (December 2001)

Inferred pressure gradient and fluid flow in a condensing sessile droplet based on the measured thickness profile

Physics of Fluids (June 2004)

12 January 2026 12:01:33

AIP Publishing

The Journal of Chemical Physics

Special Topics Open for Submissions

Learn More

AIP Publishing

A generalized van der Waals model for solvation forces between solute particles in a colloidal suspension

Ben C. Freasier

Department of Chemistry, Faculty of Military Studies, University of New South Wales, Duntroon, ACT 2600, Australia

Sture Nordholm

Department of Theoretical Chemistry, University of Sydney, Sydney, NSW 2006, Australia
(Received 19 October 1982; accepted 5 April 1983)

A model for solvation forces between two solute particles in a colloidal suspension is solved within the framework of the generalized van der Waals model (GvdW) of fluids. The results for this approximation are compared to machine simulations for a subcritical solvent. Density profiles, adsorption excess, and force of interaction are studied. Particular attention is paid to the phenomenon of liquid film formation between the particles as a function of interparticle distance. Theory and simulation are found to be in good overall agreement.

I. INTRODUCTION

A problem of outstanding importance in the theory of liquids or dense fluids is the determination of the structural (or solvation) force induced between two solute particles by the action of the medium. Various aspects of this problem is discussed in the literature on hydrophobic interactions[1,2] and on the electrostatic[3] and steric stabilization[4] of colloid dispersions. Recently it has become possible to directly measure the force between mica plates in aqueous electrolytes[5] and other liquids.[6] From a fundamental theoretical point of view it is essential to first resolve the structural forces in simple fluids before taking on the many additional complexities of realistic solvents. Calculations of structural forces in simple fluids have recently been carried out using integral equation and mean field methods.[7,2] However, it is clear that the problem makes exceptional demands upon the currently favored methods of liquid state physics and much work on simple model fluids remains to be done. At the moment it would seem that Monte Carlo simulation offers the most reliable means of studying structural forces in simple fluids. Several accounts of such simulations have appeared in the literature within the last few years.[8–13] Thus reliable predictions may now be attainable but a more analytical explanation in terms of a clear physical mechanism is still needed.

The main aim of this work is to test the utility of the generalized van der Waals (GvdW) theory, set out in a recent series of articles[14–21] in the field of solvation interactions. The demands upon a theory are of two kinds: qualitative and quantitative. In the first application we shall focus primarily on qualitative aspects of solvation forces leaving the quest for optimal accuracy for subsequent work. In their Monte Carlo simulation of structural forces between colloid particles in the large radius limit Lane and Spurling[11] discovered a very interesting film formation and snapping phenomenon when the solvent was argon gas and the colloid particles were modeled as a LJ (12-6) continuum of carbon dioxide. The simulation was carried out at a temperature about 20% below the critical temperature of argon. When the colloid particle surfaces were separated by a short distance, a liquid film would form a bridge between the particles. As the distance increased this film would suddenly snap to be replaced by a region of gas with adsorption to the extent of about one monolayer found at each surface. Lane and Spurling[22] have identified this phenomenon as a new type of surface transition. It will be our aim here to investigate this transition using the GvdW theory and offer a simple physical explanation for its existence.

In the next section the required GvdW free energy density functional and basic theory of the fluid between two plates problem will be set out. The heart of the problem is the determination of an optimized particle density profile by minimization of the free energy functional. The numerical implementation, calculations, and results are described in Secs. III and IV. A notable feature is the discovery of the local free energy minima corresponding to metastable configurations of the system. Our results and their relationship to those of Lane and Spurling[11] are discussed and conclusions drawn in the final section.

II. BASIC THEORY

We shall accept the model defined by Lane and Spurling[11] without change. The colloid particles in the infinite radius limit can be thought of as macroscopic plates inserted in a solvent. It is not necessary to consider edge effects. Instead we assume the plates to be effectively infinitely large on a microscopic length scale and the fluid will be taken to have planar symmetry parallel to the plates. Nevertheless the plates are macroscopically finite and placed in an infinite solvent medium at fixed temperature. The infinite volume ensures that the chemical potential remains at the bulk value while the plate separation is changed. Alternatively one could consider a large but finite volume where the chemical potential is kept fixed by other means, e.g., varying the particle number or the volume, but the infinite volume picture is preferred in the GvdW theory. Given these model assumptions the calculation

12 January 2026 12:01:33

 0021-9606/83/214431-08$02.10 © 1983 American Institute of Physics

can be confined to the state of the fluid between the plates and the rest of the system serves as a reservoir supplying or accepting particles at a given chemical potential.

In this model each plate will be taken to be a LJ (12-6) continuum with interaction parameters chosen to correspond to solid carbon dioxide. The solvent is fluid argon. If we let the plates be assigned the index 1 and the solvent 2 then the parameters in the LJ (12-6) pair potential

$$\phi(r) = 4\varepsilon[(\sigma/r)^{12} - (\sigma/r)^6] \tag{1}$$

are as follows:

$$\epsilon_{11} = 195.5\ k_B K \quad \sigma_{11} = 4.06\ \text{Å},$$

$$\epsilon_{22} = 119.76\ k_B K \quad \sigma_{22} = 3.405\ \text{Å},$$

$$\epsilon_{12} = 153\ k_B K \quad \sigma_{12} = 3.73\ \text{Å}.$$

The density of CO_2 molecules in the plates is taken to be $n_P = 1.274/\sigma_{11}^3$. The surfaces of the plates will be taken to be parallel to the x, y plane and located at 0 and h in the z coordinate which measures distances orthogonal to the plate surfaces. The potential exerted by the plates upon an argon atom in between them is given by a sum of potentials from each plate,

$$V_{ex}(z) = w(z) + w(h - z), \tag{2}$$

where

$$w(z) = n_p \int_{-\infty}^{z} d1 \int_0^{\infty} ds\, 2\pi s\ 4\epsilon_{12}\{[\sigma_{12}^{12}/(1^2+s^2)^6] - [\sigma_{12}^6/(1^2+s^2)^3]\} = 2\pi\sigma_{12}^3\ \epsilon_{12}\ n_p[\tfrac{2}{45}(\sigma_{12}/z)^9 - \tfrac{1}{3}(\sigma_{12}/z)^3]\,. \tag{3}$$

The potential of interaction between the two plates is

$$V_{pp}(h) = A\ n_p \int_h^{\infty} dz\, 2\pi\ \sigma_{11}^3\ \epsilon_{11}\ n_p[\tfrac{2}{45}(\sigma_{11}/z)^9 - \tfrac{1}{3}(\sigma_{11}/z)^3]$$

$$= A\ 2\pi\ \sigma_{11}^4\ \epsilon_{11}\ n_p^2[\tfrac{1}{180}(\sigma_{11}/h)^8 - \tfrac{1}{6}(\sigma_{11}/h)^2]\,, \tag{4}$$

and the direct force is

$$F_{pp}(h) = -\frac{\partial}{\partial h} V_{pp}(h) = A\ 2\pi\ \sigma_{11}^3\ \epsilon_{11}\ n_p^2 \times[\tfrac{2}{45}(\sigma_{11}/h)^9 - \tfrac{1}{3}(\sigma_{11}/h)^3]\,. \tag{5}$$

Here A is the total area of plate surface.

In the presence of the solvent an additional force, the structural or solvation force, will be acting on the plates. The simplest way to understand this is to consider the effect of the plates upon the free energy of the solvent. Suppose that the Helmholtz free energy of the solvent when the plates are at zero separation is $F(0)$. Then the free energy at separation h is

$$F(h) = F(0) + \Delta F(h)\,, \tag{6}$$

where $\Delta F(h)$ is the change in the free energy of the medium as a function of h. The solvation force will then be given by

$$F_s(h) = -\frac{\partial}{\partial h}\Delta F(h)\,. \tag{7}$$

It should be noted that in classical statistical mechanics as adopted here the momentum variables are independent and therefore make a constant contribution to the Helmholtz free energy. The value of this constant is trivially estimated but irrelevant here since we are only interested in the dependence of the free energy on h. Thus the aim of our work will be to estimate $\Delta F(h)$ from which the solvation force can be obtained. In the process we will obtain a density profile $\tilde{n}(z, h)$ describing the density of argon atoms between the plates at separation h. This profile can be identified as liquidlike or gaslike by examination of its structure a few argon diameters away from each surface.

The GvdW theory, which we shall use to calculate ΔF and $\tilde{n}$, exists in several forms. The choice of theory is made on the basis of a balance between simplicity and accuracy. Here we shall use the simple fine-grained GvdW theory wherein the hard-sphere radius is fixed at σ in the case of LJ (12-6) interactions and the excluded volume per particle v_0 is estimated to be σ^3. Thus the hard-sphere part of the free energy analysis is crude but reasonable and the use of a fine-grained functional allows sharp structures and nonlocal entropy effects to be resolved to semiquantitative accuracy.[14,16] The same theory that we shall use here has previously been successfully applied to the prediction of adsorption profiles at a LJ (12-6) wall (i.e., the single plate problem)[19] and to the study of gas/liquid interfaces in LJ (12-6) fluids.[20] The full three dimensional configurational free energy functional is given by

$$F_c(\tilde{n}) = -k_B T \int d\mathbf{r}\, \tilde{n}(\mathbf{r})\, \ln[(1 - \bar{n}(\mathbf{r})v_0)/\tilde{n}(r)] + \frac{1}{2}\int d\mathbf{r}\, d\mathbf{r}'\, \tilde{n}(\mathbf{r})\tilde{n}(\mathbf{r}')\ \phi_s(|\mathbf{r}-\mathbf{r}'|) + \int d\mathbf{r}\, \tilde{n}(\mathbf{r})\ V_{ex}(\mathbf{r})\,, \tag{8}$$

where $\tilde{n}(r)$ is the fine-grained particle density, $\bar{n}(\mathbf{r})$ is the coarse-grained particle density,

$$\bar{n}(\mathbf{r}) = (\tfrac{3}{4}\pi\sigma^3)\int d\mathbf{r}'\, n(\mathbf{r}'), \quad |\mathbf{r}-\mathbf{r}'| < \sigma\,, \tag{9}$$

and $\phi_s(r)$ is the soft part of the pair potential. In the present case we have $\phi_s(r) = 0$, $r \le \sigma$,

$$= 4\epsilon[(\sigma/r)^{12} - (\sigma/r)^6], \quad r > \sigma\,. \tag{10}$$

$V_{ex}(\mathbf{r})$ is the external potential. It will be defined by Eq. (2) in the present work.

The calculation of $\Delta F(h)$ for the present model can be simplified in two ways. First we note that changing h will change the particle number and the volume of the bulk fluid not between the plates. The corresponding change in free energy is directly related to the chemical potential μ and the pressure P of the bulk fluid and need not be calculated by way of the functional (This change in the bulk free energy can be easily derived from the Taylor series of the bulk free energy in the particle number and plate separation.) Secondly, the planar symmetry allows us to reduce out the x, y integrations in the functional. Thus we obtain

12 January 2026 12:01:33

$$\Delta F(h)/A = -k_B T \int_0^h dz\, \tilde{n}(z, h) \ln[(1-\bar{n}(z, h)v_0)/\tilde{n}(z, h)] + \frac{1}{2}\int_0^h dz\, \tilde{n}(z, h) \int_0^h dz\, \tilde{n}(z', h)\, \phi_{s1}(|z-z'|) + \int_0^h dz\, \tilde{n}(z, h)\, V_{ex}(z) - \hat{\Gamma}\mu_\beta + Ph \,, \tag{11}$$

where

$$\tilde{n}(z, h) = (\tfrac{3}{4}\sigma_{22}^3) \int_{L(z)}^{R(z)} dz'\, \tilde{n}(z', h)[\sigma_{22}^2 - (z-z')^2] \,,$$

$$R(z) = \min(z+\sigma_{22}, h) \,,$$

$$L(z) = \max(z-\sigma_{22}, h) \,, \tag{12}$$

$$v_0 = \sigma_{22}^3 \,, \tag{13}$$

$$\phi_{s1}(z) = -6\pi\epsilon_{22}\sigma_{22}^2/5, \quad |z| \le \sigma_{22} \,,$$

$$= 4\pi\epsilon_{22}\sigma_{22}^2[\tfrac{1}{5}(\sigma_{22}/z)^{10} - \tfrac{1}{2}(\sigma_{22}/z)^4], \quad |z| > \sigma_{22} \,. \tag{14}$$

The bulk free energy per particle is

$$f_\beta = -kT \ln[(1-nv_0)/n] + E_{s22}\, n/2 \tag{15}$$

and where n is the bulk particle density and $E_{s22}/2$ is the binding energy per particle,

$$E_{s22} = -32\pi\epsilon_{22}\sigma_{22}^3/9 \,. \tag{16}$$

We then readily obtain the pressure and chemical potential as ($v = n^{-1}$)

$$P = -\frac{\partial}{\partial v} f_B(n) = [K_B T/(v-v_0)] + (E_{s22}/2v^2) \,, \tag{17}$$

$$\mu = \frac{\partial}{\partial N} N f_B = f_B + vP \,. \tag{18}$$

Finally, the adsorption per unit area,

$$\hat{\Gamma} = \int_0^h dz\, \tilde{n}(z, h) \,. \tag{19}$$

Note that $\hat{\Gamma}$ is the total adsorption between the plates. We have not subtracted out the bulk gas part of the particle number per unit area, nor divided by two since there are two surfaces. The usual excess adsorption per unit area of each surface would then be obtained as

$$\Gamma = (\hat{\Gamma} - nh)/2 \,. \tag{20}$$

The solvation force is most straightforwardly obtained by direct numerical differentiation of $\Delta F(h)$ as in Eq. (7). However, it is possible to proceed by a different method proposed by Barker[8] and adopted by van Megen and Snook.[8] If we rewrite $\Delta F(h)$ as

$$\frac{\Delta F(h)}{A} = \int_0^h dz\, g[\tilde{n}(z, h),\ V_{ex}(z, h)] + Ph \,, \tag{21}$$

then the solvation force can be written as

$$F_s(h)/A = -P - g[\tilde{n}(h, h),\ V_{ex}(h, h)] - \int_0^h dz \left\{ \left[\frac{\partial}{\partial h}\tilde{n}(z, h)\right]\left(\frac{\partial}{\partial \tilde{n}} g\right) + \left[\frac{\partial}{\partial h} V_{ex}(z, h)\right]\left(\frac{\partial}{\partial V_{ex}} g\right)\right\} \,. \tag{22}$$

However, if $\tilde{n}$ is the optimal (equilibrium) profile then we have

$$\tilde{n}(0, h) = \tilde{n}(h, h) = 0 \,, \tag{23}$$

$$g[\tilde{n}(h, h),\ V_{ex}(h, h)] = 0 \,, \tag{24}$$

$$\frac{\partial}{\partial \tilde{n}} g = 0, \quad 0 \le z \le h \,, \tag{25}$$

and we get

$$F_s(h) = -P - \int_0^h dz\, \tilde{n}(z, h) \frac{\partial}{\partial h} V_{ex}(z, h) \,. \tag{26}$$

This is the Barker expression for the solvation force. It applies within the framework of GvdW theory and will lead to exactly the same prediction as the free energy derivative as long as a fully optimized particle density has been obtained. Under normal circumstances the profile obtained is, of course, not fully optimized and the two predictions may disagree to some extent. Since the free energy is the more fundamental quantity it would then seem safer to use the direct free energy derivative expression for the force if possible. The agreement between the two expressions for the force can also be used as a test of the degree of convergence and numerical accuracy of the optimization. A similar choice between a direct thermodynamic derivative and expressions involving the assumption of particle densities satisfying equilibrium constraints occur in many other applications of statistical mechanics, e.g., in the evaluation of surface tension.[21]

It should be noted that most optimization procedures search out a stationary point of the functional or a minimum but can not be trusted to choose the absolute minimum if there are other minima available in the set of possible configurations of the system. Thus independent means may have to be used to distinguish between stable and metastable configurations. Since the GvdW theory is inherently a theory of fluctuations it is well suited to studies of metastability while other theories based more rigorously on the assumption of stable equilibrium may encounter difficulties. As will be discussed in more detail below we have, in fact, discovered what appear to be long lived metastable configurations in the present problem. It is worth noting here that the derivation of Barker's force which shows the final expression to be valid also will be valid for the prediction of a metastable force, i.e., it would still agree with the direct derivative prediction (7).

III. METHOD

We now proceed to find solutions for $\tilde{n}(z)$ which minimize $F(h)/A$ as defined by Eq. (11). This procedure is implemented operationally by taking the functional derivative of Eq. (11) with respect to $\tilde{n}(z)$. This leads to the following nonlinear equation for $\tilde{n}(z)$:

$$n(z) = [1-\bar{n}(z)]\exp\left\{-\left[\int_0^h n(z')\phi_{s_1}(z-z')dz' + V_{ex}(z) - \mu\right]\Big/T - 1 - \frac{3}{4\sigma_{22}^3}\int_{L(z)}^{R(z)} dz' \frac{\tilde{n}(z')}{1-\bar{n}(z')}[\sigma_{22}^3 - (z-z')^2]\right\} \,. \tag{27}$$

The bulk density, temperature, and wall separation are

12 January 2026 12:01:33

input as parameters into the computer program. The wall-fluid potential given by Eq. (3) is assumed to be infinite when the distance between the wall and the medium particle is less than 0.7 σ_{22}. In all of the cases examined the $n(z)$ calculated at this hard core cutoff has been less than 1×10^{-5} in scaled units which is of the order of the accuracy of the calculation. We have found than an integration grid of 0.05 σ_{22} was the best compromise between accuracy and economy. The quadrature error (associated with the trapezoidal rule) was typically less than 1% in the free energy.

We performed successive iteration for $\tilde{n}(z)$ using Eq. (27) until the absolute value of the functional derivative from which Eq. (27) was derived was less than $1\times10^{-5}\ \epsilon_{22}\sigma_{22}^3$. If on a given interation the free energy from the new density profile was found to be greater than the free energy obtained from the previous trial solution, the iteration was repeated with more of the old solution mixed into the new trial solution. In any event, on each iteration at least half of the old solution was mixed into the new trial solution.

The rate of convergence and the computational time of each profile depended strongly upon the temperature, the plate separation, and the thermodynamic state of the medium between the plates. As the separation between the plates increased the iteration time per step increased basically as the plate separation squared because of the convolution integral. The liquid profiles usually took longer to converge because of the increased structure in the profiles. Low temperature profiles generally took longer for the same reason. Convergence generally took 50 to 200 iterations with a typical solution being generated in about one minute CPU time on a DEC10 with a KL10 processor.

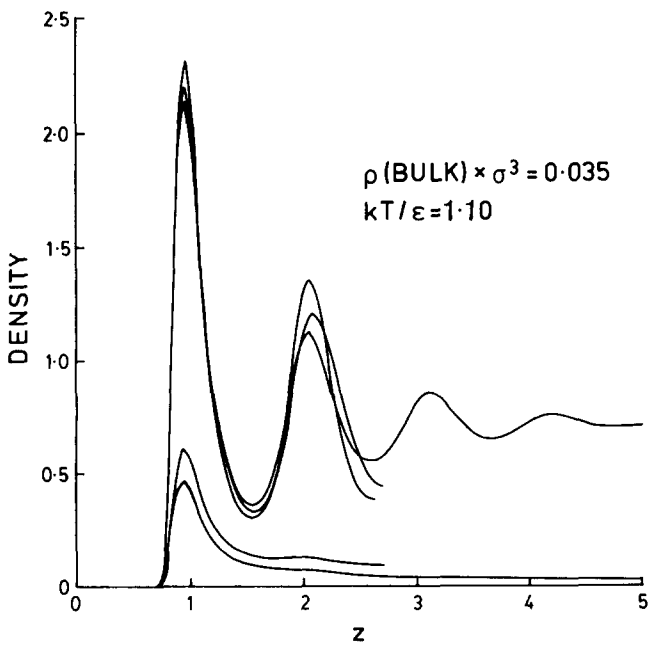

FIG. 1. Density profiles as a function of distance from the wall for a number of plate separations when the bulk reduced density is fixed at 0.035 and the bulk reduced temperature equals 1.10.

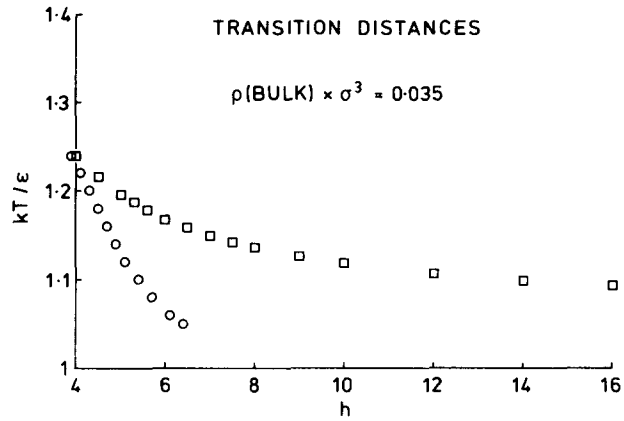

FIG. 2. Squares denote the locus of points separating liquid states from gaseous states for a number of temperatures in the bulk with the bulk reduced density equal to 0.035. The circles mark the limit of gas metastable states achieved numerically.

Before discussing the solutions generated in greater detail, we will make a few remarks about the initial trial solutions. Most frequently, the initial trial solution was given by

$$\tilde{n}(z) = n_{\mathrm{BULK}} \exp[-V_{ex}(z)/kT] \ . \tag{28}$$

This choice of trial solution favors the gas phase, and, in fact, as we shall see later, we can often calculate metastable gas phase solutions from this initial density profile. However, if the temperature and the plate separation are small enough, it is possible to realize a stable liquid solution from the initial trial solution given by Eq. (28). These generated liquid solutions can then be used to calculate other liquid solutions by appropriate perturbation. We used two different techniques. Most commonly, we increased the plate separation holding the temperature and the bulk density constant. Hence to derive a liquid solution from a previous liquid solution at a smaller plate separation, we simply used the algorithm:

$$\tilde{n}_{\mathrm{new}}(z) = \tilde{n}_{\mathrm{old}}(z), \quad z \le \frac{h_{\mathrm{old}}}{2},$$

$$\tilde{n}_{\mathrm{new}}(h_{\mathrm{new}} - z) = \tilde{n}_{\mathrm{old}}(h_{\mathrm{old}} - z), \quad h_{\mathrm{new}} - \frac{h_{\mathrm{old}}}{2} \le z \le h_{\mathrm{new}},$$

$$\tilde{n}_{\mathrm{new}}(z) = \tilde{n}_{\mathrm{old}}\left(\frac{h_{\mathrm{old}}}{2}\right), \quad \frac{h_{\mathrm{old}}}{2} < z < h_{\mathrm{new}} - \frac{h_{\mathrm{old}}}{2} \ . \tag{29}$$

A number of these profiles are displayed for $kT/\epsilon_{22} = 1.1$ and $n\sigma_{22}^3 = 0.035$ in Fig. 1 for stable liquid and metastable gas states. Rather than use Eq. (29), we could use the liquid trial solution as if we were simply working at a different temperature and/or bulk density if the plate separation was the same. This was often done in mapping the phase information displayed in Fig. 2.

IV. RESULTS

Using the numerical procedure outlined in the previous section we were able to calculate medium density profiles between the two plates. Given this microscopic

12 January 2026 12:01:33

information we can calculate surface thermodynamic information which is directly comparable to the simulation work of Lane and Spurling.[11,22]

The first point of interest is that (in common with the GvdW equation for the bulk fluid in the coexistence region) multiple solutions can be derived from Eq. (27). Reference to Fig. 1 clearly shows that the profiles can either exhibit gaseous or liquid type solutions. In fact for $kT/\epsilon_{22}=1.1$ and $n\sigma_{22}^3=0.035$ the generalized van der Waals model for the bulk fluid predicts that the bulk fluid itself is inside the coexistence region. For a given plate separation we can see that there are multiple solutions. We are also able to find a liquid type solution for large plate separations. It turns out that all of the gaseous solutions in Fig. 1 are metastable (have a higher free energy than the liquid state solutions).

A more global picture of this aspect of the result is apparent upon careful scrutiny of Fig. 2. The squares represent the boundary between gas and liquid solutions as a function of temperature and plate separation for a fixed bulk density in the reservoir. The circles represent the limit of metastable gas solutions (at least for our calculational algorithm) for a fixed plate separation. There are a few features worth nothing. Below a certain temperature (approximately $kT/\epsilon_{22}=1.1$) for a fixed bulk density of $0.035\sigma_{22}^{-3}$ the medium is always liquid regardless of the value of the plate separation. Addition of an attractive external field to a bulk fluid in a subcritical gaseous phase may well provide enough negative internal energy to force the fluid into the liquid phase. This attractive field is precisely what the two plates can often provide. Below this temperature the liquid film will never "snap". At sufficiently high temperatures ($kT/\epsilon_{22}>1.24$) still below the generalized van der Waals critical temperature the attractive walls do not provide sufficient negative internal energy to overcome the decrease in entropy associated with forming the film on the wall; hence, the medium fluid will always be in the gaseous phase.

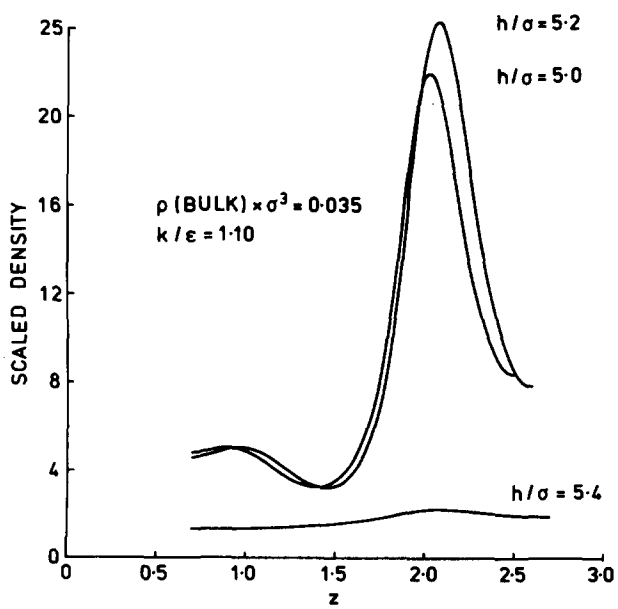

FIG. 3. Scaled density profiles according to Eq. (27) for various plate separations with a fixed reduced bulk density of 0.035 and a reduced temperature of 1.1.

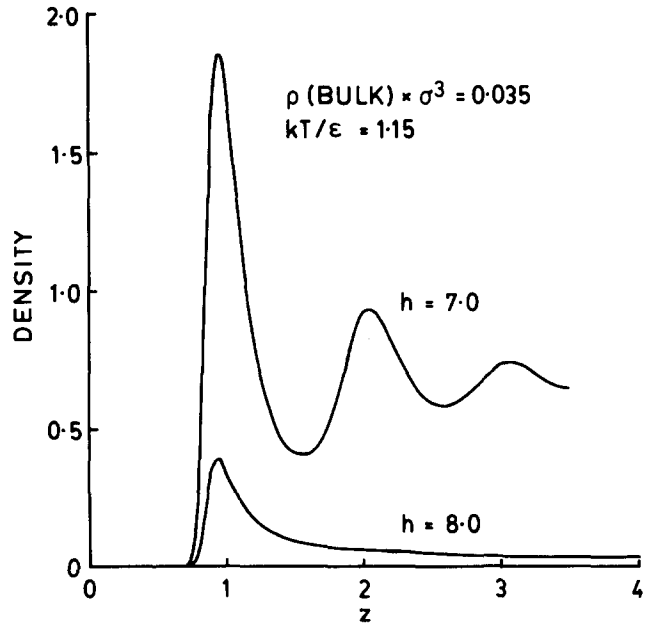

FIG. 4. Two density profiles as a function of distance from the wall for a number of plate separations when the bulk reduced density is 0.035, and the bulk reduced temperature is 1.15.

Figure 3 is designed to illustrate the difference in liquid and gas profiles at $kT/\epsilon_{22}=1.1$. Instead of plotting the density profiles, we have plotted the scaled particle densities by dividing out the explicit contribution of the wall potential to the singlet distribution function:

$$\tilde{n}_{\text{scaled}}(z)=\tilde{n}_{\text{bulk}}(z)/\exp[-V_{ex}(z)/kT]\ . \tag{30}$$

This procedure should more clearly illustrate the effect of the medium–medium correlations. Indeed, we find that the liquid profiles show greatly enhanced correlations between the medium particles adsorbed on the wall and the nearest neighbor shell in the fluid. This is particularly evident when compared to the metastable gas solution at $h=5.4\ \sigma_{22}$. Figures 4 and 5 show the same trend at a slightly higher temperature, but in Fig. 4 the gaseous density profile shown is stable.

There are also some macroscopic properties of interest. Figure 6 shows the free energy given by Eq. (11) for $kT/\epsilon_{22}=1.2$ at various plate separations. The gas branch is given by the relatively horizontal curve extending from about 4.5 to 6 σ_{22}. The other free energy curve represents the liquid branch. Their intersection is clearly the "coexistence distance" for that bulk density and temperature. The entire manifold of such intersection points are given by the squares in Fig. 1 when the bulk density is fixed at $0.035\sigma_{22}^{-3}$. It is on the basis of these plots that we were able to determine the stable phase of our numerical solutions for the density profiles.

12 January 2026 12:01:33

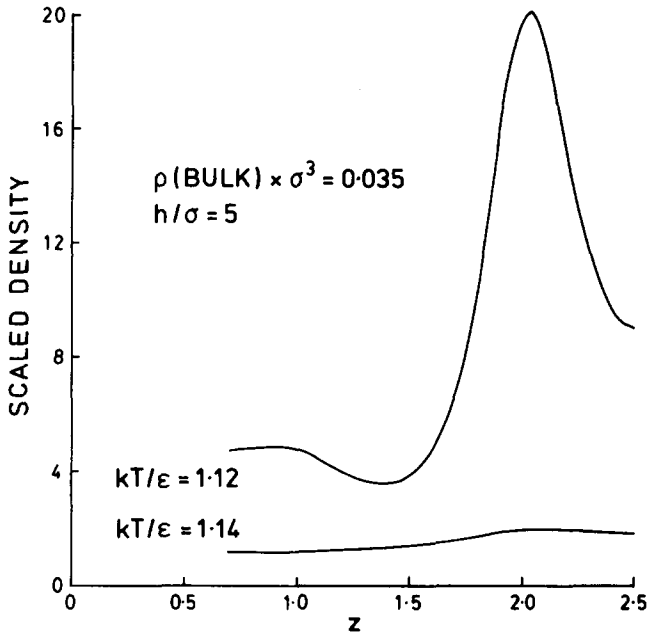

FIG. 5. Two density profiles for a fixed plate separation and varying temperature (fixed reduced density = 0.035).

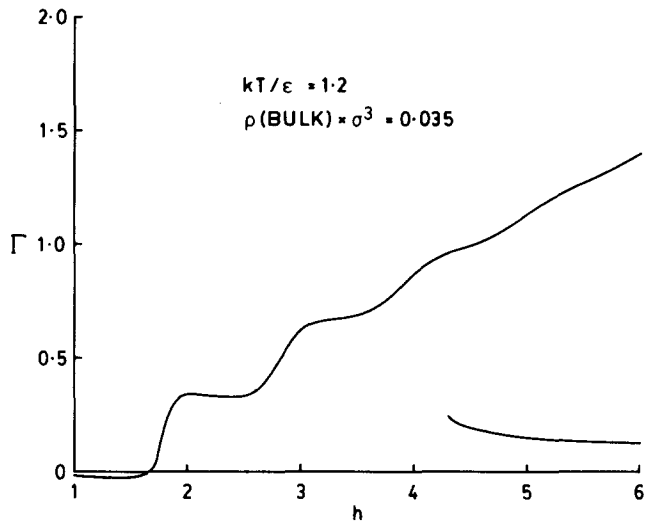

FIG. 7. Excess adsorption of medium given by Eq. (20) for bulk reduced temperature of 1.2 and a bulk reduced density of 0.035 which shows both gas and liquid phases.

Once we calculated the profiles and identified the phases we then proceeded to calculate excess adsorptions per Eq. (20). This we have done in Fig. 7 for $kT/\epsilon_{22} = 1.2$. The liquid excess adsorption shows an oscillatory behavior due to alternating constructive and destructive interference associated with the buildup of nearest neighbor shells in the liquid medium. At approximately $4.3\sigma_{22}$ the gaseous phase becomes more favored so that the excess adsorption becomes much less structured. As defined in Eq. (20) the excess adsorption will eventually go to a small single wall value for infinite plate separations. The negative adsorption at very close plate separations is due to the fact that the plates are essentially excluding all particles from the inter-plate region.

We were also able to calculate the forces as previously covered in the discussion leading to the relevant expression Eq. (26). The force calculated from Eq. (26) and found from numerically differentiation of Eq. (11) generally agreed within 1%. This is shown in Fig. 8 for $kT/\epsilon_{22} = 1.2$. The oscillations in the solvation force for the liquid branch again mimic the al-

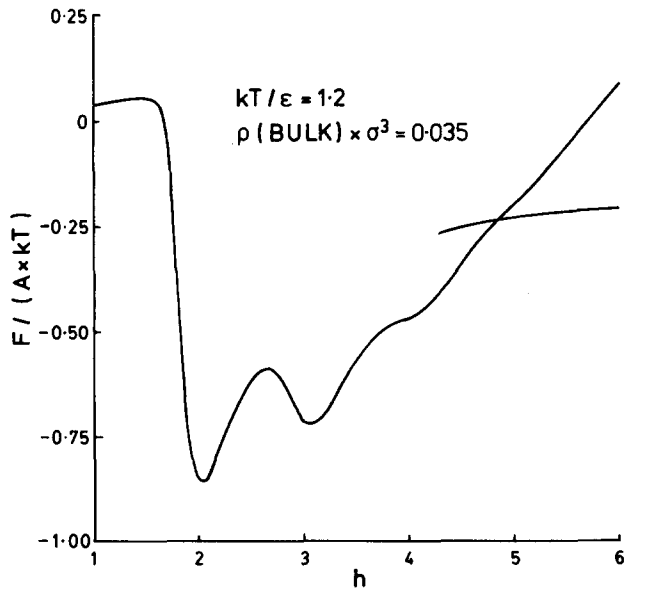

FIG. 6. Free energy of medium given by Eq. (11) for a bulk reduced temperature of 1.2 and a bulk reduced density of 0.035 which shows both gas and liquid phases.

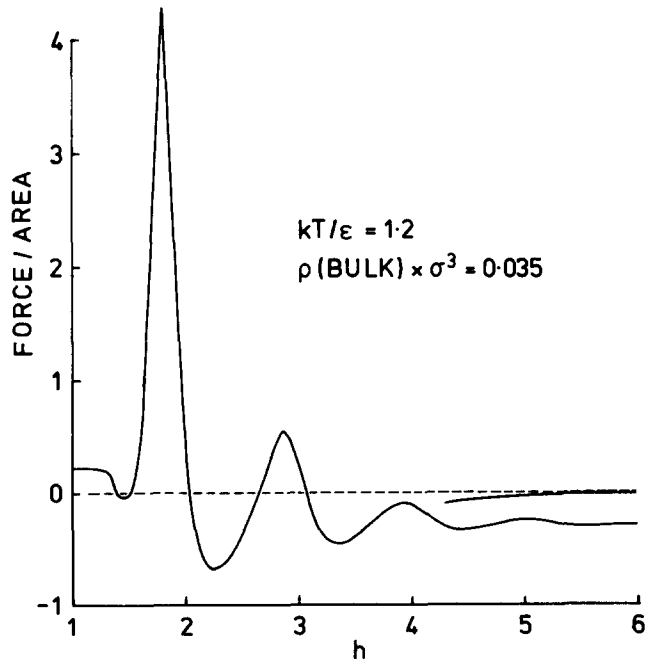

FIG. 8. Solvation force given by Eq. (26) for a bulk reduced temperature of 1.2 and a bulk reduced density of 0.035 which shows both gas and liquid phases.

12 January 2026 12:01:33

ternating buildup and broadening of the nearest neighbor shells in the liquid density profiles. The variation in the force for the gaseous branch is, as expected, not nearly so great as for the liquid. The force should go to zero, as defined in Eq. (26), which it certainly is doing in the gaseous branch. The liquid branch will not (as is shown clearly in Fig. 8) because it is trying to approach the metastable liquid density instead of the correct stable gaseous density.

Ultimately, of course, we wish to test our theory against the most accurate results available. We have directed our work towards the same model used by Lane and Spurling in their work on a model argon–carbon dioxide solid system. There are a number of items that we can compare to their work, but the most revealing would be the density profiles, the excess adsorption, and the solvation force. Lane and Spurling did their calculations at $kT/\epsilon_{22} = 1.1$ and $\rho\sigma_{22}^3 = 0.035$. Unfortunately, this phase point is just slightly inside the coexistence curve for bulk fluid in the GvdW approximation. However, if we are just interested in looking at the liquid phase, we can always just look at the liquid branch which will be the most stable branch anyway. In any event when the shift in free energy due to the attractive walls is large compared to the medium–medium forces the errors in the GvdW bulk equation of state are somewhat mitigated.

We have not displayed all of the singlet distribution functions published by Lane and Spurling. This is basically because the scale of their figures was such that quantitative comparison was somewhat risky. However, we found very similar structures (same number and relative size of peaks) at similar plate separations. The main qualitative differences that we found were that our peaks were lower and broader than theirs because the GvdW model generally underestimates the medium–medium correlations in the fluid. We have been using one of the simpler versions of the GvdW model in attempting to solve this difficult inhomogeneous problem, but there exist other versions of the model which are more accurate. For example, this version of the model does not estimate the hard core entropy (which can be dependent on temperature and density) as accurately as possible.[18]

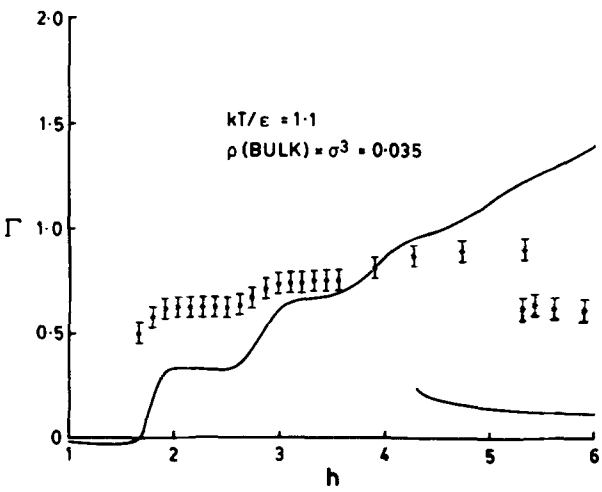

FIG. 9. Excess adsorption of medium given by Eq. (20) for a bulk reduced temperature of 1.1 and a bulk reduced density of 0.035 which shows both metastable gas and stable liquid phases.

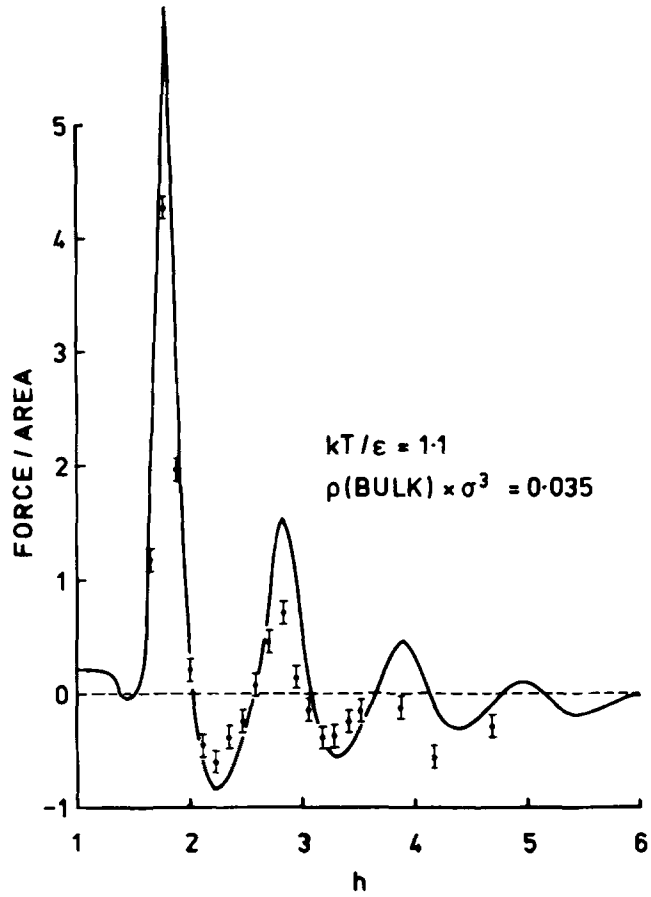

FIG. 10. Solvation force given by Eq. (20) for a bulk reduced temperature of 1.1 and a bulk reduced density of 0.035 which shows both metastable gas and stable liquid phases.

Of more direct interest perhaps is the excess adsorption. We have compared Lane and Spurling's results with ours, and these results are displayed in Fig. 9. The GvdW results are clearly too small. This is basically due to the fact that the GvdW theory underestimates the medium–medium correlations. However, the structure is very similar. We have also plotted the GvdW metastable gas phase results for comparison to Lane and Spurling's gas phase data.

The most interesting results that we have to report are for the solvation forces. The GvdW theory results are displayed with Lane and Spurling's data in Fig. 10. Considering the level of approximation involved in this version of the GvdW theory, the comparison is very favorable. The position of the first few peaks are in good agreement. There is eventually a phase difference in the later peaks because of the incorrect hard core diameter for these temperatures in this version of the GvdW model.

12 January 2026 12:01:33

V. CONCLUSION

We have solved the two plate problem in the generalized van der Waals approximation. The potential parameters describing the plates and the fluid were those used by Lane and Spurling[11] in their simulation of an argon–solid carbon dioxide system. The GvdW model qualitatively predicts the correct behavior of the solvation force, the excess adsorption, and the singlet distribution functions. We are also able to predict the gas–liquid phase transition associated with varying the plate separation while keeping the bulk temperature and density constant which Lane and Spurling first discovered. The ability of the GvdW theory to predict the solvation forces so accurately is extremely significant. As far as we know, this is the only theory capable of predicting the simulation results for the solvation force which can be of such importance in colloidal dispersions. In fact, considering the level of approximation in the GvdW theory and the theoretical difficulty of solving inhomogeneous problems, the agreement of the GvdW theory with most of the Lane and Spurling data is excellent.

As the GvdW is a physical theory, it is often possible to interpret the result in terms of physical concepts. The liquid forms because the attractive wall potential effectively shifts the local chemical potential to a new value equal to the sum of the bulk gas value and the wall potential. This decrease in chemical potential leads to an increase in local density particularly where the external field (wall potential) is the most attractive, namely, close to the wall. Nevertheless, at sufficiently small separation, a liquid will be condensed to fill the entire region between the plates. As the plates are drawn apart, this liquid bridge will persist until the free energy cost of establishing two gas–liquid surfaces is less than can be gained by the decrease in internal energy associated with the medium particles being close to each other in a liquid type conformation.

In the process of solving this problem we have discovered metastable gas phase solutions to the GvdW equations which bear a resemblance to Lane and Spurling's phase results at $kT/\epsilon_{22} = 1.1$. Our stable profiles at this temperature disagree with those of Lane and Spurling by being liquidlike at all relevant separations. This may be due to the error in the bulk phase diagram as obtained from our GvdW theory for this fluid, but one must also consider whether the Monte Carlo transition might have been from a metastable state. One way to ensure that the real thermodynamic transition has been located is to run Monte Carlo simulations long enough that both structures and transitions in both directions can be observed in a single trajectory. Note that a metastable transition ought to be irreversible. The bimodal distribution of particle number observed by Lane and Spurling[11] would seem to indicate that they have indeed observed the thermodynamic transition. Nevertheless observations of metastability are likely in these and other similar circumstances. We feel that it is one of the strengths of the GvdW theory that it can resolve such phenomena. It seems likely that GvdW theory can be a useful tool for the investigation of solvation forces between colloidal particles.

ACKNOWLEDGMENTS

We would like to acknowledge the ARGS for their support of this work. In addition we would like to thank Dr. Lane, Dr. Spurling, Dr. van Megen, and Dr. Snook for early reprints of their simulation work. Finally, we would like to acknowledge the stimulating discussions held at the Australian National University in the Applied Mathematics Department without which this work would never have been done.

[1] A. Ben-Naim, *Hydrophobic Interactions* (Plenum, New York, 1980).
[2] D. Y. C. Chan, D. J. Mitchell, B. W. Ninham, and B. A. Pailthorpe, in *Water: A Comprehensive Treatise*, edited by F. Franks (Plenum, New York, 1979), Vol. 6, Chap. 5.
[3] E. J. W. Verwey and J. Th. G. Overbeek, *Theory of Stability of Lyophobic Colloids* (Elsevier, Amsterdam, 1948).
[4] D. H. Napper, J. Colloid Interface Sci. **58**, 390 (1977).
[5] J. N. Israelachvilli and G. E. Adams, J. Chem. Soc. Faraday Trans. 2 **74**, 975 (1978).
[6] R. G. Horn and J. N. Israelachvilli, Chem. Phys. Lett. **71**, 192 (1980).
[7] D. Y. C. Chan, D. J. Mitchell, B. W. Ninham, and B. A. Pailthorpe, Mol. Phys. **35**, 1669 (1978); Chem. Phys. Lett. **56**, 533 (1978); J. Chem. Soc. Faraday Trans. 2 **75**, 556 (1979).
[8] W. van Megen and I. Snook, J. Chem. Soc. Faraday Trans. 2 **75**, 1095 (1979).
[9] J. E. Lane and T. H. Spurling, Chem. Phys. Lett. **67**, 107 (1979).
[10] I. K. Snook and W. van Megen, J. Chem. Phys. **72**, 2907 (1980).
[11] J. E. Lane and T. H. Spurling, Aust. J. Chem. **33**, 231 (1980).
[12] W. van Megen and I. K. Snook, J. Chem. Phys. **74**, 1409 (1981).
[13] I. K. Snook and W. van Megen, J. Chem. Phys. **75**, 4738 (1981).
[14] S. Nordholm and A. D. J. Haymet, Aust. J. Chem. **33**, 2013 (1980).
[15] M. A. Hooper and S. Nordholm, Aust. J. Chem. **33**, 2029 (1980).
[16] S. Nordholm, M. Johnson, and B. C. Freasier, Aust. J. Chem. **33**, 2139 (1980).
[17] S. Nordholm, B. C. Freasier, N. D. Hamer, and D. L. Jolly, Chem. Phys. **47**, 347 (1980).
[18] M. A. Hooper and S. Nordholm, Aust. J. Chem. **34**, 1809 (1981).
[19] M. Johnson and S. Nordholm, J. Chem. Phys. **75**, 1953 (1981).
[20] S. Nordholm and J. Gibson, Aust. J. Chem. **34**, 2263 (1981).
[21] S. Nordholm, J. Gibson, and M. A. Hooper, J. Stat. Phys. **28**, 391 (1982).
[22] J. E. Lane and T. H. Spurling, Aust. J. Chem. **34**, 1529 (1981).

12 January 2026 12:01:33